



# Combustion kinetics of the coke on deactivated dehydrogenation catalysts



Sha Luo<sup>a,b</sup>, Songbo He<sup>a,c,\*</sup>, Xianru Li<sup>a,b</sup>, Jingqiu Li<sup>a</sup>, Wenjun Bi<sup>a</sup>, Chenglin Sun<sup>a,\*\*</sup>

<sup>a</sup> Dalian National Laboratory for Clean Energy, Dalian Institute of Chemical Physics, Chinese Academy of Sciences, Dalian 116023, PR China

<sup>b</sup> University of Chinese Academy of Sciences, Beijing 100049, PR China

<sup>c</sup> Catalytic Processes and Materials, MESA + Institute for Nanotechnology, University of Twente, P.O. Box 217, 7500 AE Enschede, The Netherlands

## ARTICLE INFO

### Article history:

Received 30 April 2014

Received in revised form 27 August 2014

Accepted 3 September 2014

Available online 24 September 2014

### Keywords:

Kinetics

Coke combustion

Deactivation

Long chain paraffin

Dehydrogenation

Pt–Sn catalysts

## ABSTRACT

The coke combustion kinetics on the deactivated catalysts for long chain paraffin dehydrogenation was studied by the thermogravimetry and differential thermogravimetry (TG–DTG) technique. The amount and H/C mole ratio of the coke were determined by the TG and elemental analysis. And the comprehensive coke combustion model and catalytic combustion mechanism were also proposed. The results showed that three types of coke existed, which were located on the metal sites (C1) and the support sites surrounding (C2) and far from Pt (C3), respectively. The reaction order with respect to carbon was 1, 1/3 and 3/4, and to oxygen was 0, 1/2 and 3/4, respectively for the coke C1, C2 and C3. Moreover, the corresponding activation energy was 31, 107 and 127 kJ/mol, respectively.

© 2014 Elsevier B.V. All rights reserved.

## 1. Introduction

Dehydrogenation of long chain paraffins to olefins is an important step in linear alkylbenzene sulfonate production, which is extensively employed for biodegradable detergents, hydraulic oils, flotation and oil recovery agents [1]. The Pt–Sn/Al<sub>2</sub>O<sub>3</sub> catalysts are widely used in the industrial process of long chain paraffin dehydrogenation. Some literatures about the effect of the additives and supports on the Pt–Sn/Al<sub>2</sub>O<sub>3</sub> catalysts have been reported [2–4]. However, the life-time of the commercial catalysts for long chain paraffin dehydrogenation, such as DEH, NDC and DF types of catalysts, is only 40–60 days [5]. Some papers showed that the coke formed on the catalyst surface during the dehydrogenation process, which led to the deactivation of the catalysts [6–9]. Sahoo et al. [10] found that the coke deposited on the deactivated catalysts for long chain paraffin dehydrogenation consisted of soluble and insoluble coke. The former was mostly composed of polymerized aromatic and aliphatic hydrocarbons and the latter was mainly comprised of polycyclic aromatic hydrocarbons. He et al. [11] indicated that the coke gradually accumulated on the catalyst surface during the dehydrogenation of long chain paraffins. With the prolongation of the

reaction, the graphitization degree of the coke was increased, but the formation rate was decreased. Generally, the deactivated catalysts can be regenerated by coke combustion, which is the most effective method for the decoking treatment. The coke combustion process is highly exothermic, and the temperature jump can lead to the damage of the catalyst structure [12,13]. Consequently, it is very important to optimize the process. Numerous papers regarding the coke combustion conditions have been published [14–16]. Afonso et al. [17] reported that the rapid heating rate and high combustion temperature must be avoided, but the combustion time should be long enough during the regeneration process of Pt–Sn/Al<sub>2</sub>O<sub>3</sub> catalysts. The appropriate conditions were: heating rate 2 °C/min, temperature 450 °C and time 8 h, respectively. Barbier et al. [18] observed that the coke deposited on the metal sites could be removed when the combustion temperature was 270 °C for the Pt–Re/Al<sub>2</sub>O<sub>3</sub> and Pt–Ir/Al<sub>2</sub>O<sub>3</sub> catalysts. However, temperature higher than 400 °C was required to eliminate the coke located on the support sites. In our previous work, the coke combustion procedures of the deactivated catalysts for long chain paraffin dehydrogenation have been investigated [19]. It was suggested that the deactivated catalysts were treated initially in O<sub>2</sub>/N<sub>2</sub> containing 1 vol.% O<sub>2</sub> for 3 h, then in O<sub>2</sub>/N<sub>2</sub> containing 3 vol.% O<sub>2</sub> for 2 h, and finally in air for 3 h. Moreover, the combustion temperature and gas hourly space velocity (GHSV) were controlled at 500 °C and 1000 h<sup>−1</sup>, respectively.

Kinetic study about the combustion of coke on the deactivated catalysts is essential to the simulation of the regeneration process. Some investigations about the coke combustion kinetics on the cracking and

\* Correspondence to: S. He, Dalian National Laboratory for Clean Energy, Dalian Institute of Chemical Physics, Chinese Academy of Sciences, Dalian 116023, PR China. Tel.: +31 68 1746818.

\*\* Corresponding author. Tel.: +86 411 84379133.

E-mail addresses: [songbohe@gmail.com](mailto:songbohe@gmail.com) (S. He), [clsun@dicp.ac.cn](mailto:clsun@dicp.ac.cn) (C. Sun).

reforming catalysts have been reported [20–24]. The coke combustion kinetics on the cracking catalysts was proposed to be first-order with respect to carbon and approximately first-order with oxygen [25]. However, the coke combustion kinetics on the dehydrogenation catalysts has not yet been reported. The characteristics of the coke deposited on such catalysts are quite different from that on the cracking catalysts, and thus the coke combustion kinetics is distinct. The purpose of this work is to study the coke combustion kinetics on the deactivated catalysts for long chain paraffin dehydrogenation, and the catalytic combustion mechanism will be also proposed.

## 2. Experimental

### 2.1. Deactivated catalyst sample

The fresh Pt–Sn–K/Al<sub>2</sub>O<sub>3</sub> catalysts, with the component of Pt 0.5 wt.%, Sn 1.5 wt.% and K 0.5 wt.%, were obtained from PetroChina Fushun Petrochemical Company, PR China. The dehydrogenation reaction of long chain paraffins was performed under industrial conditions, and the deactivated catalysts were discharged after a 45-day continuous run. The n-paraffins were industrial grade n-C<sub>10</sub>–C<sub>13</sub> which were used in the industrial PACOL plant. The component was n-C<sub>10</sub> 11.67 wt.%, n-C<sub>11</sub> 29.37 wt.%, n-C<sub>12</sub> 32.29 wt.%, n-C<sub>13</sub> 26.25 wt.% and n-C<sub>14</sub> 0.07 wt.%. The reaction conditions were as follows: pressure 0.14 MPa, liquid hourly space velocity of n-paraffins 20 h<sup>-1</sup>, and gas hourly space velocity of hydrogen 12,000 h<sup>-1</sup>. The reaction temperature was increased from 473 °C stepwise up to 479 °C to maintain a certain conversion. The TG results showed that the coke deposited on the deactivated catalysts was 4.5 wt.%.

### 2.2. Elemental analysis

The amount of C and H elements of the coke was determined using a Vario EL III Universal CHNOS Elemental Analyzer (Elementar Analysensysteme GmbH, Hanau, Germany). The samples were oxidized in pure oxygen (99.995%) at 1150 °C. The results showed that the H/C mole ratio of the coke on the deactivated catalysts was 1.8.

### 2.3. TG–DTG experiments

The TG–DTG experiments of the deactivated catalysts were performed on a thermogravimetric analysis instrument (SETSYS 16/18, France). The samples with the weight of 10.0 mg were heated from ambient temperature to 600 °C at a heating rate of 10 °C/min. The gas flow rate was 100 mL/min.

### 2.4. Coke combustion experiments

The coke combustion experiments were performed on the same apparatus as the TG–DTG experiments. In order to eliminate the effect of the internal diffusion on the intrinsic kinetics, the deactivated catalysts were ground and sieved to 100–120 mesh based on Eq. (1) [26].

$$N_{W-P} = \frac{R_{O_2} \rho_0 L_0^2}{D_{e,O_2} (C_{O_2})_s} \ll 1 \quad (1)$$

where  $N_{W-P}$ ,  $R_{O_2}$ ,  $\rho_0$ ,  $L_0$ ,  $D_{e,O_2}$  and  $(C_{O_2})_s$  represent the Weisz–Prater criterion, the observed reaction rate of oxygen, the density of the catalyst, the diameter of the catalyst particle, the effective diffusivity of oxygen, and the oxygen concentration at the particle surface, respectively.

After being purged in N<sub>2</sub> under the specified temperature, the burning gas was switched from N<sub>2</sub> to O<sub>2</sub>/N<sub>2</sub> mixed gas containing 0.8–21 vol.% O<sub>2</sub>. The oxygen partial pressure was varied by adjusting the volume ratio of oxygen to nitrogen, and the gas flow rate was kept at 100 mL/min during the whole process. The weight percentage of the

samples was recorded as a function of the coke combustion time until no weight loss.

## 3. Results and discussion

### 3.1. Characterization of the deactivated catalysts

The TG–DTG profiles of the deactivated catalysts are plotted in Fig. 1. Four distinct peaks were identified from the DTG curve. The peaks located at about 100 °C and 250 °C were attributed to the removal of weakly adsorbed steam and hydrocarbons. The peaks around 450 °C and 520 °C were generally related to the combustion of coke deposited on the active metal and support sites [27,28]. Based on the TG curve, these two types of coke were approximately 68 wt.% and 32 wt.% of the total coke. In this paper, we mainly focus on these two kinds of coke.

### 3.2. Coke combustion kinetics

The coke deposited on the deactivated catalysts was primarily composed of the element carbon and small amounts of hydrogen. Carbon rich in hydrogen could be completely removed in the earliest minutes [29], and therefore the total reaction rate nearly reflected the combustion of coke in oxygen, which could be expressed by Eq. (2) or Eq. (3).

$$r = -\frac{dC_C}{dt} = kP_{O_2}^m C_C^n \quad (2)$$

$$\ln r = \ln k + m \ln P_{O_2} + n \ln C_C \quad (3)$$

where  $C_C$ ,  $P_{O_2}$ ,  $k$ ,  $m$  and  $n$  represent the coke concentration, the oxygen partial pressure, the rate constant, and the reaction order with respect to oxygen and carbon. When  $P_{O_2}$  and  $T$  are constant, Eq. (3) can be shortened as Eq. (4) where  $\ln K = \ln k + m \ln P_{O_2}$ .

$$\ln r = \ln K + n \ln C_C. \quad (4)$$

### 3.3. Parameter estimation

#### 3.3.1. Effect of the coke concentration

The reaction order with respect to carbon was investigated by the coke combustion experiments at different temperatures and is displayed in Fig. 2. All the experiments were performed at the same oxygen partial pressure of 8.7 kPa. The coke combustion reaction was considered to be nearly isothermal due to small amounts of the coked samples. High gas flow rate kept the oxygen partial pressure approximately constant before and after the experiment.

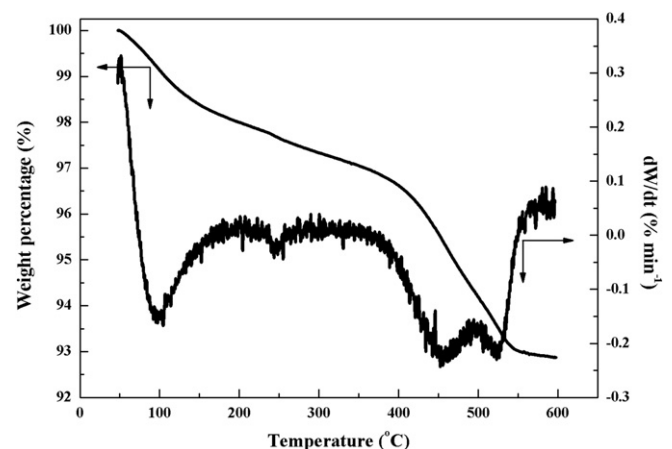


Fig. 1. TG–DTG profiles of the deactivated catalysts.

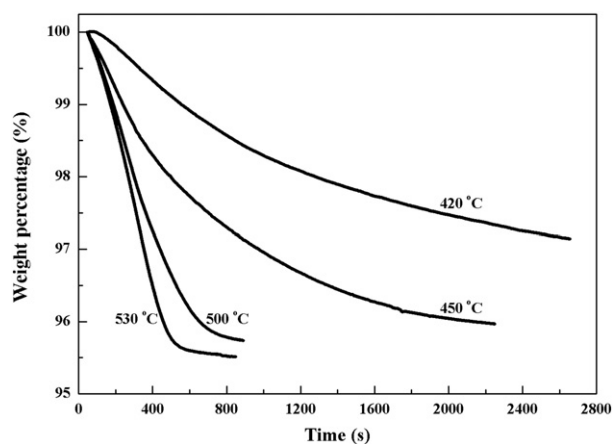


Fig. 2. TG profiles of the deactivated catalysts at different combustion temperatures.

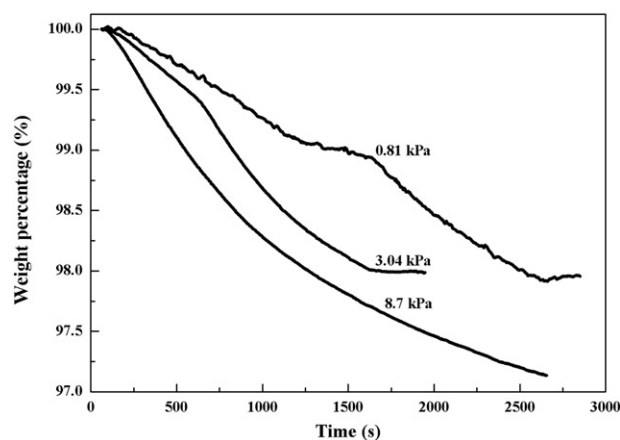


Fig. 3. TG profiles of the deactivated catalysts at different oxygen partial pressures under 420 °C.

The coke combustion rate was found to be rapidly increased in the initial minutes and then gradually decreased to zero. It was also observed that the coke combustion at 420 °C was incomplete. Approximately 64 wt.% of the total coke was burned off, in accordance with the coke amount on the metal sites calculated from Fig. 1. The initially removed coke might be attributed to the carbon rich in hydrogen, and it was approximately 4 wt.% of the total coke. However, the combustion rate of such coke was difficult to measure accurately, and therefore it was not taken into account. Additionally, two distinct zones with different slopes were observed corresponding to 320–1000 s and 1000–2500 s, which were attributed to the combustion of the carbon C1 and C2, respectively. Moreover, it was discovered that these two types of coke could be completely eliminated under this condition, and the difference depended on their combustion activity.

Most of the coke could be removed at 500 °C, and three distinct zones with different slopes were seen corresponding to 270–400 s, 400–500 s and 500–700 s, which were attributed to the combustion of the carbon C1, C2 and C3, respectively. The carbon C3 was approximately 32 wt.% of the total coke, in accordance with the coke amount on the support sites calculated from Fig. 1. Baumgarten et al. [30] reported that the dissociative O\* chemisorbed on the active metal surface could react with the coke deposited on the metal. When the combustion temperature was increased to higher than 450 °C, the chemisorbed O\* could migrate to the surrounding support and react with the coke on it. Consequently, the carbon C1 and C2 might be attributed to the coke on the metal and the support around Pt, respectively. However, the combustion of C3 on the support sites was not influenced by the catalytic combustion of the active metal. The combustion activity order of the three types of coke was: C1 > C2 > C3, and the corresponding concentration was 38, 26 and 32 wt.%, respectively.

The experimental values were used to confirm the reaction order with respect to such three types of coke based on Eq. (4). It was obtained, according to Fig. 2, by the relationships of the reaction rate ( $\ln(-dC/dt)$ ) with the coke concentration ( $\ln C$ ) remaining on the catalysts at different temperatures. A linear correlation was well observed, and the fitted

results are summarized in Table 1. The reaction order with respect to the three types of coke was 1, 1/3 and 3/4, respectively.

### 3.3.2. Effect of the oxygen partial pressure

The reaction order with respect to oxygen was examined by the coke combustion experiments at 420 °C (Fig. 3) and 500 °C (Fig. 4). It was observed in Fig. 3 that approximately 42 wt.% of the total coke was burned off when the oxygen partial pressure was lower than 3.04 kPa, which was in accordance with the amount of the carbon rich in hydrogen and C1. It indicated that the carbon C2 and C3 had no activity under such conditions. Two distinct zones with plateau were identified, and it became less prominent with the increasing oxygen partial pressure. The two zones were ascribed to the combustion of the carbon rich in hydrogen and C1, respectively. It was seen in Fig. 4 that the coke combustion rate was remarkably influenced by the oxygen partial pressure especially when it was lower than 8.7 kPa. Consequently, it was necessary to strictly control the oxygen partial pressure during the coke combustion process.

Similarly, the reaction order with respect to oxygen was calculated at a certain coke concentration based on Eq. (3). It was obtained, according to Figs. 3 and 4, by the relationships of the reaction rate ( $\ln(-dC/dt)$ ) with the oxygen partial pressure ( $\ln P_{O_2}$ ). A linear correlation was well observed, and the fitted results are listed in Table 2. The rate constant  $k_i$  was almost the same at a given temperature regardless of the oxygen partial pressure, and the reaction order with respect to oxygen was 0, 1/2 and 3/4, respectively for the carbon C1, C2 and C3. It indicated that the combustion rate equation of the carbon C1 did not involve the oxygen partial pressure, but the carbon C2 probably reacted with the dissociative O\* migrated from the metal to the surrounding support. The reaction order for the carbon C3 was in agreement with the results reported by Haldeman et al. [31].

### 3.3.3. Effect of the combustion temperature

In order to determine the effect of the combustion temperature on the rate constant, the coke combustion experiments were performed at different temperatures. The Arrhenius curves for three types of coke,

**Table 1**  
The fitted results of the reaction order with respect to the three types of coke.

Temperature (°C)	C1		C2		C3	
	$n_1$	$\ln k_1 + m_1 \ln P_{O_2}$	$n_2$	$\ln k_2 + m_2 \ln P_{O_2}$	$n_3$	$\ln k_3 + m_3 \ln P_{O_2}$
420	0.98	-2.75	0.31	-3.02	-	-
450	0.99	-2.43	0.30	-1.81	0.79	-2.35
500	1.05	-1.31	0.31	-0.96	0.79	-0.84
530	-	-	0.38	-0.49	0.79	-0.24

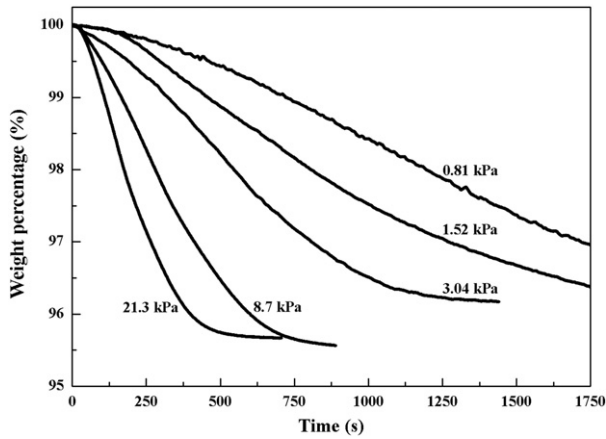


Fig. 4. TG profiles of the deactivated catalysts at different oxygen partial pressures under 500 °C.

which were obtained by the relationships of the rate constant ( $\ln k$ ) with the combustion temperature ( $1000/T$ ) based on Fig. 2, are plotted in Fig. 5. The corresponding activation energy and pre-exponential factor are listed in Table 3. The activation energy for the three types of coke was 31, 107 and 127 kJ/mol, respectively, which was in agreement with the results reported by Pieck et al. [32]. The activation energy for the carbon C2 was three times more than that for the carbon C1, indicating that the carbon C2 needed higher energy to form the activated species  $C^*$ . However, much lower energy was enough for the carbon C1 owing to the catalytic combustion effect. The activation energy for the carbon C3 was in agreement with the results reported by Weisz et al. [33].

Moreover, the pre-exponential factor for three types of coke could be well explained by the kinetic compensation effect [34,35]. The relationship curve between the pre-exponential factor and activation energy is plotted in Fig. 6, and a linear correlation was well observed. Additionally, the rate constant could be expressed by Eq. (5) where A, E, R and T represent the pre-exponential factor, activation energy, molar gas constant and temperature, respectively.

$$k = A \exp(-E/RT). \quad (5)$$

### 3.3.4. Comprehensive coke combustion model

As summarized above, the kinetic equations for the three types of coke were proposed during the combustion of coke on the deactivated catalysts for long chain paraffin dehydrogenation.

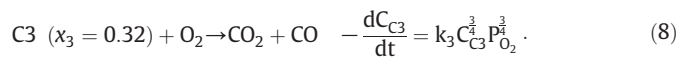
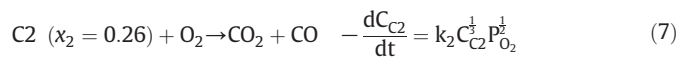
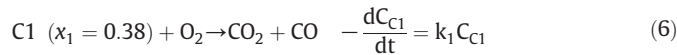


Table 2

The fitted results of the reaction order with respect to oxygen for the three types of coke.

$P_{O_2}$ (kPa)	420 °C			500 °C					
	C1	C2	C3	C1	C2	C3			
	$\ln k_1$	$m_1$	$R^2$	$\ln k_2$	$m_2$	$R^2$	$\ln k_3$	$m_3$	$R^2$
0.81	-2.98			0.81	-2.21		-1.98		
				1.52	-1.92		-2.05		
3.04	-2.95	0.06	0.99	3.04	-1.90	0.45	-2.00	0.71	0.98
				8.70	-2.06		-2.21		
8.70	-2.87			21.3	-2.02		-2.62		

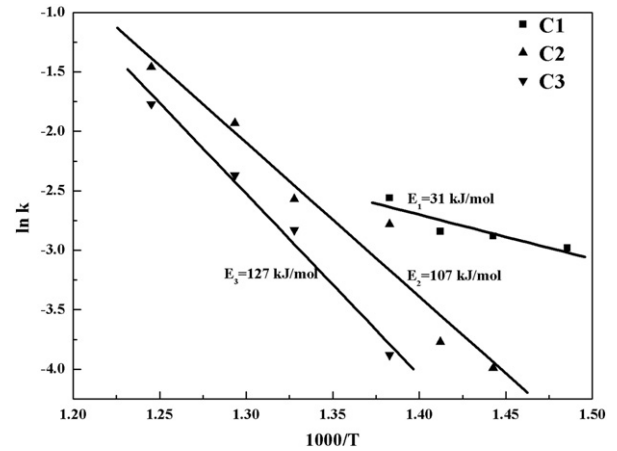


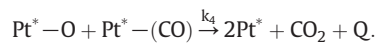
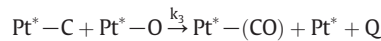
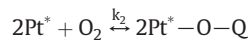
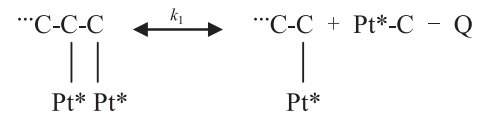
Fig. 5. Arrhenius curves of the deactivated catalysts for the three types of coke.

Generally, the total rate equation could be expressed as in the following Eq. (9).

$$\frac{dC_{C_{tot}}}{dt} = 50 \exp\left(-\frac{31,000}{RT}\right) (C_{tot} \cdot x_1) + 2.4 \times 10^6 \exp\left(-\frac{107,000}{RT}\right) P_{O_2}^{\frac{1}{2}} (C_{tot} \cdot x_2)^{\frac{1}{3}} + 3.3 \times 10^7 \exp\left(-\frac{127,000}{RT}\right) P_{O_2}^{\frac{3}{4}} (C_{tot} \cdot x_3)^{\frac{3}{4}} \quad (9)$$

### 3.4. Catalytic combustion mechanism

As mentioned above, the combustion properties of three types of coke were different due to the catalytic combustion effect. A possible mechanism was proposed as follows:



The first step was the formation of the activated carbide  $Pt^*-C$  from the catalytic cracking reaction of the bulk  $\cdots C-C-C$  chemisorbed on the metal sites. The second was the dissociative adsorption of oxygen, and its concentration depended on the oxygen partial pressure and coke combustion temperature [36]. The third was the formation of the intermediate  $Pt^*-(CO)$ , which was transformed into carbon dioxide once it collided with  $Pt^*-O$ .

Table 3

Activation energy and pre-exponential factor for the three types of coke.

Coke type	Activation energy (kJ mol <sup>-1</sup> )	Pre-exponential factor (10 <sup>5</sup> Pa) <sup>-m</sup> (min) <sup>-1</sup>	R <sup>2</sup>
C1	31	50	0.95
C2	107	2.4 × 10 <sup>6</sup>	0.98
C3	127	3.3 × 10 <sup>7</sup>	0.99



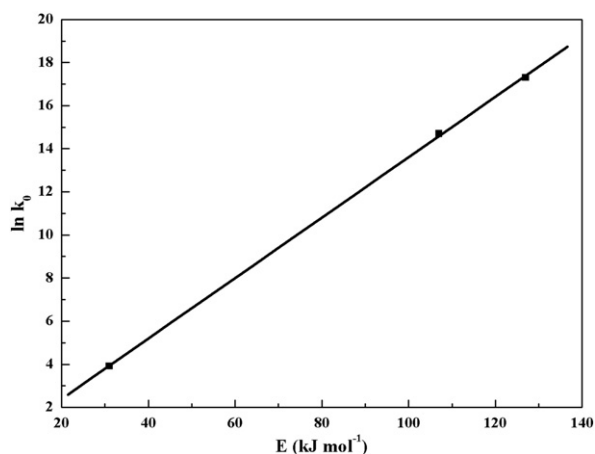


Fig. 6. Relation curve between the pre-exponential factor and activation energy.

It was concluded above that the catalytic combustion of the carbon C1 exhibited the characteristics of zero-order reaction with respect to oxygen and first-order with carbon. It indicated that the rate-determining step of the catalytic combustion reaction was the first above. Similar results have also been reported by Holstein et al. [37]. Consequently, the reaction rate equation was proposed as Eq. (10).

$$-\frac{dC_C}{dt} = k_1 C_C. \quad (10)$$

The heat flow curves at different oxygen partial pressures are plotted in Fig. 7. It was observed that the heat flow was increased obviously in the initial minutes, which resulted from the exothermic combustion of the coke ( $CH_x$ ). And then the heat flow was decreased sharply, indicating that the hydrogen-rich coke was totally eliminated but some more polymerized coke was still burning. Finally, all the coke was eliminated and the heat flow was almost zero. Moreover, a distinct plateau was seen when the oxygen partial pressure was lower than 3.04 kPa. Under such conditions, the fraction of the activated species such as  $Pt^*-O$  was lacking and thus the intermediate  $Pt^*-CO$  could not be transformed immediately. However, the activated species were increased with the increase of the oxygen partial pressure and therefore the plateau disappeared.

#### 4. Conclusion

In this work, the combustion kinetics of coke on the deactivated catalysts for long chain paraffin dehydrogenation has been investigated.

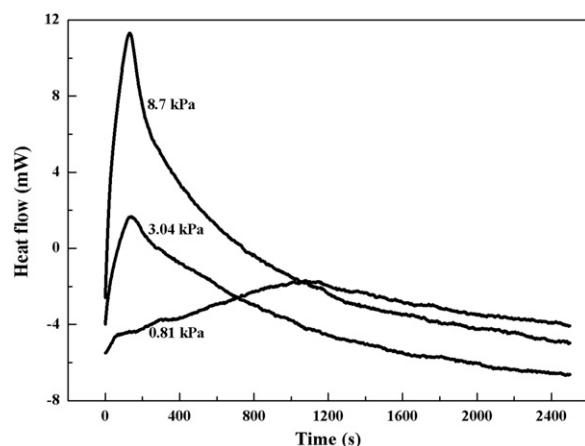


Fig. 7. Heat flow curves of the deactivated catalysts at different oxygen partial pressures under 420 °C.

It can be concluded that three types of coke, which are deposited on the metal and the support sites surrounding and far from Pt, respectively, are observed. The corresponding reaction order with respect to carbon was 1, 1/3 and 3/4, respectively. Moreover, the reaction order with oxygen was 0, 1/2 and 3/4, respectively for the carbon C1, C2 and C3. And the corresponding activation energy was 31, 107 and 127 kJ/mol, respectively.

#### Acknowledgments

The authors thank Changhai Xu for helping with the TG-DTG measurements. Financial support was provided by the Liaoning Provincial Natural Science Foundation of China (Grant No. 2013020111).

#### References

- [1] M.M. Bhasin, J.H. McCain, B.V. Vora, T. Imai, P.R. Pujado, Dehydrogenation and oxydehydrogenation of paraffins to olefins, *Applied Catalysis A: General* 221 (2001) 397–419.
- [2] S.B. He, Y.L. Lai, W.J. Bi, X. Yang, X. Rong, C.L. Sun, Effect of K promoter on the performance of Pt–Sn–K/gamma-Al<sub>2</sub>O<sub>3</sub> catalyst for n-hexadecane dehydrogenation, *Chinese Journal of Catalysis* 31 (2010) 435–440.
- [3] S.B. He, C.L. Sun, Z.W. Bai, X.H. Dai, B. Wang, Dehydrogenation of long chain paraffins over supported Pt–Sn–K/Al<sub>2</sub>O<sub>3</sub> catalysts: a study of the alumina support effect, *Applied Catalysis A: General* 356 (2009) 88–98.
- [4] A.D. Qiu, Y.N. Fan, Y.F. Ma, P.C. Wu, Y. Chen, Effects of alkali promoters on catalytic properties of alumina-supported Pt–Sn catalysts for long-chain paraffin dehydrogenation, *Chinese Journal of Catalysis* 22 (2001) 343–347.
- [5] S.B. He, Studies on the catalysts and the coke deposition behavior of the dehydrogenation of long chain paraffins (C<sub>10</sub>–C<sub>19</sub>), *Chemical Engineering, Dalian Institute of Chemical Physics, Chinese Academy of Sciences, Dalian*, 2009.
- [6] J.C. Afonso, M. Schmal, R. Frety, The chemistry of coke deposits formed on a Pt–Sn catalyst during dehydrogenation of n-alkanes to mono-olefins, *Fuel Processing Technology* 41 (1994) 13–25.
- [7] J.Q. Li, Studies on the regeneration of long-chain paraffin dehydrogenation catalyst, *Chemical Engineering, Dalian Institute of Chemical Physics, Chinese Academy of Sciences, Dalian*, 2006.
- [8] T. Zhang, Study of carbon deposition on highly dispersed Pt/Al<sub>2</sub>O<sub>3</sub> and Pt–Sn/Al<sub>2</sub>O<sub>3</sub> catalysts for dehydrogenation of alkanes, *Chemical Engineering, Dalian Institute of Chemical Physics, Chinese Academy of Sciences, Dalian*, 1989.
- [9] C.H. Bartholomew, Catalyst deactivation, *Chemical Engineering* 91 (1984) 96–112.
- [10] S.K. Sahoo, P.V.C. Rao, D. Rajeshwer, K.R. Krishnamurthy, I.D. Singh, Structural characterization of coke deposits on industrial spent paraffin dehydrogenation catalysts, *Applied Catalysis A: General* 244 (2003) 311–321.
- [11] S.B. He, C.L. Sun, X. Yang, B. Wang, X.H. Dai, Z.W. Bai, Characterization of coke deposited on spent catalysts for long-chain-paraffin dehydrogenation, *Chemical Engineering Journal* 163 (2010) 389–394.
- [12] Y.N. Fan, J.L. Zang, L.W. Lin, Effect of coking–burning off cycle on the properties of Pt/Al<sub>2</sub>O<sub>3</sub> and PtSn/Al<sub>2</sub>O<sub>3</sub> catalysts, *Chinese Journal of Catalysis* 10 (1989) 111–117.
- [13] Y.N. Fan, J.L. Zang, L.W. Lin, Effect of coking–burning off cycle on the properties of Pt/Al<sub>2</sub>O<sub>3</sub> and PtSn/Al<sub>2</sub>O<sub>3</sub> catalysts: the surface reactivity of regenerated catalysts, *Chinese Journal of Catalysis* 12 (1991) 7–13.
- [14] C.L. Pieck, C.R. Vera, C.A. Querini, J.A. Parera, Differences in coke burning-off from Pt–Sn/Al<sub>2</sub>O<sub>3</sub> catalyst with oxygen or ozone, *Applied Catalysis A: General* 278 (2005) 173–180.
- [15] T.Y. Jiang, B. Wang, X.H. Dai, Z.W. Bai, The development in the regeneration technologies for long-chain paraffin dehydrogenation catalysts, *Contemporary Chemical Industry* 34 (2005) 127–129.
- [16] E. Furimsky, Effect of oxygen concentration on temperature runaway during regeneration of hydrotreating catalyst, *Applied Catalysis* 44 (1988) 189–198.
- [17] J.C. Afonso, D.A.G. Aranda, M. Schmal, R. Frety, Regeneration of a Pt–Sn/Al<sub>2</sub>O<sub>3</sub> catalyst: influence of heating rate, temperature and time of regeneration, *Fuel Processing Technology* 50 (1997) 35–48.
- [18] J. Barbier, G. Corro, Y. Zhang, J.P. Bournville, J.P. Franck, Coke formation on bimetallic platinum rhenium and platinum iridium catalysts, *Applied Catalysis* 16 (1985) 169–177.
- [19] J.Q. Li, H.Z. Du, C.L. Sun, X.H. Dai, B. Wang, Studies on the coke burning of long-chain paraffin dehydrogenation catalyst, *Industrial Catalysis* 13 (2005) 320–324.
- [20] V.D. Dimitriadis, A.A. Lappas, I.A. Vasalos, Kinetics of combustion of carbon in carbonaceous deposits on zeolite catalysts for fluid catalytic cracking units (FCCU). Comparison between Pt and non Pt-containing catalysts, *Fuel* 77 (1998) 1377–1383.
- [21] G.X. Wang, S.X. Lin, W.J. Mo, C.L. Peng, G.H. Yang, Kinetics of combustion of carbon and hydrogen in carbonaceous deposits on zeolite-type cracking catalysts, *Industrial & Engineering Chemistry Process Design and Development* 25 (1986) 626–630.
- [22] C. Li, C. Le Minh, T.C. Brown, Kinetics of CO and CO<sub>2</sub> evolution during the temperature-programmed oxidation of coke deposited on cracking catalysts, *Journal of Catalysis* 178 (1998) 275–283.
- [23] C.A. Querini, S.C. Fung, Temperature-programmed oxidation technique – kinetics of coke O<sub>2</sub> reaction on supported metal-catalysts, *Applied Catalysis A: General* 117 (1994) 53–74.
- [24] Y. Chang, D.D. Perlmutter, Catalyst regeneration kinetics in the presence of pore blockage, *AIChE Journal* 35 (1989) 385–392.

- [25] A. Bondi, W.G. Schlaffer, R.S. Miller, Rapid deactivation of fresh cracking catalyst, *Industrial & Engineering Chemistry Process Design and Development* 1 (1962) 196–203.
- [26] P.B. Weisz, C.D. Prater, Interpretation of measurements in experimental catalysis, *Advances in Catalysis* 6 (1954) 143–196.
- [27] Z.S. Xu, J.L. Zang, T. Zhang, Study of the carbonaceous deposition on Pt/Al<sub>2</sub>O<sub>3</sub> catalysts by temperature programmed oxidation, *Chinese Journal of Catalysis* 7 (1986) 230–236.
- [28] N. Martin, M. Viniestra, R. Zarate, G. Espinosa, N. Batina, Coke characterization for an industrial Pt–Sn/gamma-Al<sub>2</sub>O<sub>3</sub> reforming catalyst, *Catalysis Today* 107–08 (2005) 719–725.
- [29] F.E. Massoth, Oxidation of coked silica–alumina catalyst, *Industrial & Engineering Chemistry Process Design and Development* 6 (1967) 200–207.
- [30] E. Baumgarten, A. Schuck, Oxygen spillover and its possible role in coke burning, *Applied Catalysis* 37 (1988) 247–257.
- [31] R.G. Haldeman, M.C. Botty, On the nature of the carbon deposit of cracking catalysts, *The Journal of Physical Chemistry* 63 (1959) 489–496.
- [32] C.L. Pieck, R.J. Verderone, E.L. Jablonski, J.M. Parera, Burning of coke on Pt–Re Al<sub>2</sub>O<sub>3</sub> catalyst – activation-energy and oxygen reaction order, *Applied Catalysis* 55 (1989) 1–10.
- [33] P.B. Weisz, R.B. Goodwin, Combustion of carbonaceous deposits within porous catalyst particles: 2. Intrinsic burning rate, *Journal of Catalysis* 6 (1966) 227–236.
- [34] T. Bligaard, K. Honkala, A. Logadottir, J.K. Norskov, S. Dahl, C.J.H. Jacobsen, On the compensation effect in heterogeneous catalysis, *Journal of Physical Chemistry B* 107 (2003) 9325–9331.
- [35] G.M. Schwab, On the apparent compensation effect, *Journal of Catalysis* 84 (1983) 1–7.
- [36] W.L. Holstein, M. Boudart, Uncatalyzed and platinum-catalyzed gasification of carbon by water and carbon-dioxide, *Journal of Catalysis* 75 (1982) 337–353.
- [37] W.L. Holstein, M. Boudart, Hydrogenolysis of carbon and its catalysis by platinum, *Journal of Catalysis* 72 (1981) 328–337.